



DR LATHA PERIYASAMY (Orcid ID : 0000-0002-6564-2026)

DR MOHANE SELVARAJ COUMAR (Orcid ID : 0000-0002-0505-568X)

Article type : Research Article

## **Title: Overcoming vincristine resistance in cancer: computational design and discovery of piperine inspired P-glycoprotein inhibitors**

**Running title:** Piperine inspired P-glycoprotein inhibitors

Safiulla Basha Syed,<sup>a,b</sup> Shu-Yu Lin,<sup>c</sup> Hemant Arya,<sup>a</sup> I-Hsuan Fu,<sup>c</sup> Teng-Kuang Yeh,<sup>c</sup> Mariasoosai Ramya Chandar Charles,<sup>a</sup> Latha Periyasamy,<sup>d</sup> Hsing-Pang Hsieh,<sup>c,e,\*</sup> and Mohane Selvaraj Coumar<sup>a,\*</sup>

<sup>a</sup>Centre for Bioinformatics, School of Life Sciences, Pondicherry University, Kalapet, Puducherry-605014, India.

<sup>b</sup>DBT-Interdisciplinary Program in Life Sciences, Pondicherry University, Kalapet, Puducherry-605014, India

<sup>c</sup>Institute of Biotechnology and Pharmaceutical Research, National Health Research Institutes, 35 Keyan Road, Zhunan, Miaoli County 350, Taiwan, ROC.

<sup>d</sup>Department of Biochemistry & Molecular Biology, School of Life Sciences, Pondicherry University, Kalapet, Puducherry- 605014, India.

<sup>e</sup>Department of Chemistry, National Tsing Hua University, Hsinchu, Taiwan, ROC.

Correspondence: mohane@bicpu.edu.in; hphsieh@nhri.org.tw

This article has been accepted for publication and undergone full peer review but has not been through the copyediting, typesetting, pagination and proofreading process, which may lead to differences between this version and the [Version of Record](#). Please cite this article as [doi: 10.1111/CBDD.13758](https://doi.org/10.1111/CBDD.13758)

This article is protected by copyright. All rights reserved

## **Acknowledgment**

This work was supported by grants from Dept. of Biotechnology, Govt. of India under DBT-IPLS program (BT/PR14554/INF/22/125/2010) and Twining program for North East (to MSC, BT/246/NE/TBP/2011/77) and Ministry of Science and Technology, Taiwan (for HPH, MOST-105-2113-M-400-003). Authors thank UGC-SAP (No.F.3-19/2012(SAP-II) for providing funds to establish a cell culture facility. SBS thanks University Grants Commission (UGC) Government of India, for JRF and SRF fellowship (20/12/2015(ii)EU-V, Roll No. 316388) and DBT-IPLS for providing fellowship and the lab facility.

## **Authors' contributions**

S.M.C., H.P.H. and S.B.S. designed the work. S.B.S. and T.K.Y. performed the *in vitro* experiments. S.B.S., H.A. and M.R.C.C performed the *in silico* experiments. I.H.F. synthesized the compounds. S.B.S. and S.M.C. wrote the manuscript. All the authors contributed to the data analysis and approved the final manuscript.

## **Conflict of interest**

Authors declare no conflict of interest.

## Abstract:

P-glycoprotein (P-gp)/MDR-1 plays a major role in the development of multidrug resistance (MDR) by pumping the chemotherapeutic drugs out of the cancer cells and reducing their efficacy. A number of P-gp inhibitors were reported to reverse the MDR when co-administered with chemotherapeutic drugs. Unfortunately, none has approved for clinical use due to toxicity issues. Some of the P-gp inhibitors tested in the clinics are reported to have cross-reactivity with CYP450 drug metabolizing enzymes, resulting in unpredictable pharmacokinetics and toxicity of co-administered chemotherapeutic drugs. In this study, two piperine analogs (**3** and **4**) having lower cross-reactivity with CYP3A4 drug metabolizing enzyme are identified as P-glycoprotein (P-gp) inhibitors through computational design, followed by synthesis and testing in MDR cancer cell lines overexpressing P-gp (KB Ch<sup>R</sup> 8-5, SW480-VCR and HCT-15). Both the analogs significantly increased the vincristine efficacy in MDR cancer cell lines at low micromole concentrations. Specifically, **3** caused complete reversal of vincristine resistance in KB Ch<sup>R</sup> 8-5 cells and found to act as competitive inhibitor of P-gp as well as potentiated the vincristine induced NF-KB mediated apoptosis. Therefore, **3** ((2*E*,4*E*)-1-(6,7-dimethoxy-3,4-dihydroisoquinolin-2(1*H*)-yl)-5-(4-hydroxy-3-methoxyphenyl)penta-2,4-dien-1-one) can serve as a potential P-gp inhibitor for *in vivo* investigations, to reverse multi-drug resistance in cancer.

**Key Words:** P-glycoprotein, multi-drug resistance, anti-cancer drug, computer-aided drug design, piperine analogs and CYP3A4

## 1. Introduction

P-glycoprotein (P-gp/*MDR-1*) belonging to the ABC family of efflux pump transporters plays an important role in the development of drug resistance in cancer (Ghaleb et al., 2018; Waghray & Zhang, 2018). From the clinical studies, it is evident that the expression of *MDR-1* is inversely proportional to the efficacy of first-line chemotherapy (Chung, Santiago, De Jesus, Trinidad, & See, 2016). Moreover, some of the clinical studies have also revealed an increased expression of P-gp after chemotherapy, which positively correlates with the relapse of the tumor (Chevillard et al., 1996; Zhou, Zittoun, & Marie, 1995). One of the strategies widely used to overcome the drug resistance in cancer is to inhibit the P-gp function and based on the pre-clinical success, many P-gp inhibitors were tested in the clinics in combination with different chemotherapeutic drugs. Unfortunately, so far none of them succeeded to reach the market, due to toxicity issues., for instance, verapamil which was majorly characterized as a calcium antagonist and later known to inhibit P-gp by competitive inhibition had dose-limiting toxicities such as hypotension, heart block, etc (Pennock et al., 1991).

We reported earlier that the P-gp inhibitors that went into clinical trials had high lipophilicity ( $\log P > 5$ ) and molecular weight ( $> 500$  Da) and therefore could possibly be the reason for their failure since these are the two major physicochemical properties taken into consideration during drug development process (Syed et al., 2017). The other major reason behind their failure was cross-reactivity with the cytochrome 450 (CYP) enzymes that catalyze the oxidative metabolism of drugs and inhibition of these enzymes affects the drug metabolism and leads to drug toxicity (Wandel et al., 1999).

To circumvent the above limitations, researchers have shown much interest in phytochemicals as lead molecules for P-gp inhibition due to the broad chemical diversity and biological potential (Abdallah, Al-Abd, El-Dine, & El-Halawany, 2015; Silva, Salgueiro, Fortuna, & Cavaleiro, 2016; Syed & Coumar, 2016). However, many of them are also reported as inhibitors of CYP enzymes (Syed & Coumar, 2016).

Piperine is one of the phytochemicals reported for P-gp modulator activity and also for CYP3A4 inhibitory activity (Bhardwaj et al., 2002). Due to the low molecular weight and known biological activities of piperine (**1**), in our previous study, two piperine analogs (**2** and related analog; **Fig. 1**) having a low molecular weight ( $< 400$  Da) and low lipophilicity ( $\log P < 4$ ) were tested for P-gp inhibitory activity. Both analogs found to revert the drug resistance, specifically, **2** was as potent as verapamil in reversing the drug resistance in multi-drug resistant (MDR) cancer

cells (Syed et al., 2017). Despite the potent activity profile, **2** at 1  $\mu\text{M}$  and 10  $\mu\text{M}$  caused 28.4% and 92.3% CYP3A4 enzyme inhibition, respectively. Whereas, piperine and verapamil at 1  $\mu\text{M}$  caused 21.7% and 24.4% enzyme inhibition, and at 10  $\mu\text{M}$  caused 83.9% and 72.4% enzyme inhibition, respectively (**Table 1**). This suggests that **2** may also interfere with the metabolism of chemotherapeutic drugs during concomitant *in vivo* administration, leading to unpredictable toxicity. Therefore, the current study was pursued to develop low molecular weight and low lipophilic piperine analogs (**Fig. 1**) based on the lead **2**, with reduced CYP3A4 enzyme inhibitory activity without compromising the P-gp inhibitory activity.

## 2. Materials and methods

### 2.1. *In silico* studies

#### 2.1.1. Molecular docking

Human P-gp (hP-gp) modelled (Syed et al., 2017) based on the P-gp of *C.elegans* (PDB ID: 4F4C) was used to for *in silico* docking studies. Compounds were docked in both the substrate binding site as well in the nucleotide binding domain 1 (NBD1) of P-gp (hP-gp) by using Glide extra precision (XP) implemented in Maestro v9.2 as, described earlier (Syed et al., 2017). To dock the compounds in the substrate binding site, residue were defined as described previously (Syed et al., 2017). To dock the compounds in the NBD1, the grid was generated by selecting the key residues (Gly427, Asn428, Ser429, Gly430, Cys431, Gly432, Lys433, Ser434, Thr435, Lue1176, Ser1177, Gly1178, Gly1179, and Gln1180) reported to bind with the ATP (Becker, Depret, Van Bambeke, Tulkens, & Prévost, 2009; Kim & Chen, 2018).

#### 2.1.2. Molecular dynamics simulation

Molecular dynamic simulations of P-gp-ligand complexes were carried out for 100 ns as described previously (Syed et al., 2017). Binding free-energy between p-gp and the inhibitors was estimated using MM-PBSA approach employing g\_mmpbsa tool (Kumari, Kumar, & Lynn, 2014). The first 20 ns of the simulation were excluded as part of extended equilibria. From the remaining trajectory, one frame for each nanosecond was extracted and a total of 81 (20-100 ns) frames were used to calculate the protein-ligand free energy. P-gp along with the membrane bilayer was considered as a receptor and the inhibitors alone as ligands. Since the inhibitors were bound in the interfacial region of the lipid bilayer, dielectric constant 8 was used to calculate the energy values and other parameters were kept default (Tian, 2010). Clustering of the trajectories

(20 ns to 100 ns) was performed for the backbone of the protein structure with an RMSD cutoff of 2.5 Å and gromos method using gmx cluster tool in GROMACS. The cluster centre from the most populated clusters was used as the representative structure to compare with the initial and final conformations of protein-ligand complexes.

## 2.2. Synthesis of piperine analogs

### 2.2.1. (2E,4E)-5-(4-hydroxy-3-methoxyphenyl)-2,4-pentadi-enoic acid (8)

To a solution of 4-hydroxy-3-methoxycinnamaldehyde (**6**, 356.3 mg, 2.0 mmol) in pyridine (30 ml) was added malonic acid (**7**, 458.3 mg, 4.5 mmol) and piperidine (3.0 ml), and stirred at reflux for 1.0 h. After the reaction mixture was cooled to room temperature, it was quenched with HCl<sub>(aq)</sub> (pH 2). The solution was extracted with chloroform and ethyl acetate, dried over MgSO<sub>4</sub>, filtered, and concentrated in vacuum to give a solid residue. The crude solid was washed with dichloromethane to give the desired product **8** (218.7 mg, 50%). <sup>1</sup>H NMR (300 MHz, DMSO-*d*<sub>6</sub>) δ 9.44 (br s, 1H), 7.32–7.25 (m, 1H), 7.16 (d, *J* = 1.8 Hz, 1H), 6.99–6.91 (m, 3H), 6.76 (d, *J* = 8.1 Hz, 1H), 5.90 (d, *J* = 15.3 Hz, 1H), 3.81 (s, 3H).

### 2.2.2. (2E,4E)-5-(3,4-dihydroxyphenyl)-2,4-pentadienoic acid (9)

To a solution of compound **8** (130 mg, 0.590 mmol) in dichloromethane (3.0 ml) was added 1.0 M boron tribromide solution in dichloromethane (2.95 ml, 2.95 mmol) in ice bath. After the reaction mixture was stirred for 2.5 h, it was quenched with ice water and extracted with ethyl acetate. The organic layer was dried over Na<sub>2</sub>SO<sub>4</sub>, filtered, and concentrated to give the desired product **9** (125 mg, quantitative yield) which was used for the next step without further purification. <sup>1</sup>H NMR (300 MHz, DMSO-*d*<sub>6</sub>) δ 12.09 (br s, 1H), 9.37 (s, 1H, OH), 9.07 (s, 1H, OH), 7.29 (dd, *J* = 15.0 & 10.5 Hz, 1H), 6.94–6.71 (m, 5H), 5.90 (d, *J* = 15.0 Hz, 1H); LC-MS (ESI) *m/z*: 229.1 [M + Na]<sup>+</sup>.

### 2.2.3. (2E,4E)-1-(6,7-dimethoxy-3,4-dihydroisoquinolin-2(1H)-yl)-5-(4-hydroxy-3-methoxyphenyl)penta-2,4-dien-1-one (3)

A solution of compound **8** (50.0 mg, 0.227 mmol), 1-hydroxybenzotriazole hydrate (HOBt, 32.6 mg, 0.241 mmol), and N,N'-diisopropylcarbodiimide (DIC, 30.4 mg, 0.241 mmol) in dichloromethane (23 ml) was stirred at room temperature for 15 min. Triethylamine (33.5 μl, 0.241 mmol) and 6,7-dimethoxy-1,2,3,4-tetrahydroisoquinoline hydrochloride (**10**, 55.4 mg, 0.241

mmol) were added to the mixture. After the reaction mixture was stirred at room temperature for 6 h, it was treated with ethyl acetate, water, and  $\text{NH}_4\text{Cl}_{(\text{aq})}$ . The isolated organic layer was washed with water and brine, dried over  $\text{Na}_2\text{SO}_4$ , filtered, and concentrated to give a residue. The residue was purified by flash column chromatography (33–100% ethyl acetate in hexanes) to give the desired product **3** (63.2 mg, 70%) as a solid.  $^1\text{H}$  NMR (400 MHz,  $\text{CDCl}_3$ )  $\delta$  7.52–7.47 (m, 1H), 7.03–6.96 (m, 2H), 6.90 (d,  $J = 8.4$  Hz, 1H), 6.81–6.90 (m, 1H), 6.80 (d,  $J = 2.0$  Hz, 1H), 6.66–6.60 (br m, 2H), 6.50 (d,  $J = 14.8$  Hz, 1H), 5.74 (s, 1H), 4.75–4.70 (br m, 2H), 3.94 (s, 3H), 3.93–3.80 (m, 8H), 2.90–2.80 (br m, 2H); LC-MS (ESI)  $m/z$ : 396.3  $[\text{M} + \text{H}]^+$ ; HPLC purity = 95.4%.

#### **2.2.4. (2E,4E)-1-(6,7-dimethoxy-3,4-dihydroisoquinolin-2(1H)-yl)-5-(3,4-dihydroxy phenyl) penta-2,4-dien-1-one (4)**

A solution of compound **9** (125 mg, 0.606 mmol), 1-hydroxybenzotriazole hydrate (HOBt, 86.8 mg, 0.642 mmol), and DIC (81 mg, 0.642 mmol) in dichloromethane (61 ml) in DMF (2.0 ml) was stirred at room temperature for 30 min and then added triethylamine (89.5  $\mu\text{l}$ , 0.642 mmol) and **10** (147 mg, 0.642 mmol). After the reaction mixture was stirred at room temperature for 6 h, it was treated with ethyl acetate, water, and  $\text{NH}_4\text{Cl}_{(\text{aq})}$ . The isolated organic layer was washed with water and brine, dried over  $\text{Na}_2\text{SO}_4$ , filtered, and concentrated to give a residue. The residue was purified by flash column chromatography (50% ethyl acetate in hexanes) to give the desired product **4** (23.1 mg, 10%) as a solid.  $^1\text{H}$ -NMR (300 MHz,  $\text{CD}_3\text{OD}-d_4$ )  $\delta$  7.39 (dd,  $J = 14.7, 9.6$  Hz, 1H), 6.98 (d,  $J = 1.8$  Hz, 1H), 6.92–6.73 (m, 6H), 6.67 (d,  $J = 14.7$  Hz, 1H), 4.76–4.70 (br m, 2H), 4.06–3.87 (m, 2H), 3.82 (s, 3H), 3.81 (s, 3H), 2.87–2.81 (m, 2H); LC-MS (ESI)  $m/z$ : 382.2  $[\text{M} + \text{H}]^+$ ; HPLC purity = 95.1%.

### **2.3. In vitro studies**

#### **2.3.1. Materials**

Verapamil hydrochloride, piperine, vincristine sulfate, dimethyl sulfoxide (DMSO), RIPA buffer, and protease inhibitor cocktail were purchased from Sigma-Aldrich, USA. Primary antibody anti- $\alpha$ -tubulin was purchased from Santa Cruz Biotechnology (Santa Cruz, CA, USA). Anti-NF $\kappa$ B p65, anti-phospho-NF $\kappa$ B (Ser536), anti-PARP and cleaved PARP (Asp214) were purchased from Cell Signaling Technology (Beverly, MA, USA). Secondary antibodies horseradish peroxidase conjugated anti-mouse IgG and anti-rabbit IgG were purchased from Santa Cruz Biotechnology (Santa Cruz, CA, USA) and Cell Signaling Technology (Beverly, MA, USA),

respectively. P-gpGlo assay system was purchased from Promega Corporation (USA). All other cell culture chemicals and reagents were purchased from HiMedia (Mumbai, India).

### **2.3.2. CYP3A4 enzyme inhibition assay**

To examine the inhibition of CYP3A4 by piperine analogs, baculovirus-insect cell-expressed human CYP3A4 enzyme was used. The assay was performed according to the procedure described by Yao et al. (Yao, Chang, Lan, & Yeh, 2008; Yao et al., 2007). Briefly, the assay was done in a 96-well plate with an overall reaction volume of 0.2 ml consisting of potassium phosphate buffer (84 mM; pH 7.4), 3 mM magnesium chloride ( $\text{MgCl}_2$ ), 3 mM NADPH, CYP3A4 enzyme (100 pmol/ml), testosterone (60  $\mu\text{M}$ ; probe substrate for CYP3A4) and 1  $\mu\text{M}$  or 10  $\mu\text{M}$  of azamulin/verapamil/piperine/piperine analogs. Methanol was used as the vehicle for dissolving the compounds and the final volume was not exceeded 1% (v/v). The reaction mixture without P-gp modulators (containing only the vehicle) was used as the control. The reaction mixture was incubated aerobically at 37 °C for 60 min with constant shaking in a temperature controlled heating block. After 60 min of incubation, the reaction was stopped by adding 200  $\mu\text{l}$  of ice-cold acetonitrile. Later, the samples were vortexed and centrifuged at 20,800g for 20 min at room temperature. Finally, the supernatant (20  $\mu\text{l}$ ) was analyzed for testosterone and its metabolites formation by LC-MS and LC-MS/MS.

### **2.3.3. Cell culture**

Human KB-3-1, KB Ch<sup>R</sup> 8-5, SW480 and HCT-15 cells were obtained from the National Centre for Cell Science (NCCS, Pune, India). The resistant KB Ch<sup>R</sup> 8-5 was maintained in 10 nM of colchicine and SW80-VCR cells were developed and cultured as described previously (Syed et al., 2017). The passage number 25-30 was used for KB 3-1 and KB Ch<sup>R</sup> 8-5 cell line, passage number 35-40 was used for SW480 and SW480-VCR cells and passage number 42- 45 was used for HCT-15 cells.

### **2.3.4. Cell viability assay**

MTT (3-(4,5-Dimethylthiazol-2-yl)-2,5-diphenyltetrazolium bromide) assay was done as described previously (Syed et al., 2017). Fold-resistance (FR) was calculated by dividing the  $\text{IC}_{50}$  of vincristine in parental cells and resistant cells in the absence or presence of P-gp inhibitors by  $\text{IC}_{50}$  value for vincristine in parental cells. Fold-resistance reversal (FRR) was calculated by

dividing the FR value for vincristine alone by FR value for vincristine in the presence of P-gp inhibitors.

### 2.3.5. P-gp ATPase activity assay

The P-gp ATPase activity was assessed using P-gpGlo assay system (catalog# V3601, Lot# 0000232087) by following the protocol provided by the supplier (Promega Corporation, USA). Briefly, in a 96 well plate, 20  $\mu$ l of different drugs (2.5x concentrated) were incubated with 20  $\mu$ l of recombinant human P-gp (25  $\mu$ g) in a membrane fraction at 37 °C for 5 minutes. Later, the reaction was initiated by adding 10  $\mu$ l of 25 mM Mg ATP to all wells and incubated for 40 minutes at 37 °C in dark. Sodium orthovanadate ( $\text{Na}_3\text{VO}_4$ ) was used as the P-gp ATPase inhibitor. DMSO was used as a vehicle to dissolve the compounds and final concentration was not exceeded above 0.2%. The reaction mixture without any drug served as control. Later, the reaction was stopped and luminescence was initiated by adding 50  $\mu$ l of ATP detection reagent to all wells. The plate was further incubated for 20 minutes at room temperature. The luminescence developed was read by a luminescence detector (Molecular Devices, USA).

The average relative light units (RLU) were taken to compare the change in ATPase activity. Basal P-gp ATPase activity ( $\Delta\text{RLU}_{\text{basal}}$ ) was calculated by the following formula:

$$\Delta\text{RLU}_{\text{basal}} = \text{RLU}_{\text{Na}_3\text{VO}_4} - \text{RLU}_{\text{NT}}$$

Where  $\text{RLU}_{\text{Na}_3\text{VO}_4}$  is the average luminescent light units from  $\text{Na}_3\text{VO}_4$  treated sample and  $\text{RLU}_{\text{NT}}$  is the average luminescent light units from untreated samples (control).

Similarly, the P-gp ATPase activity in the presence of test compound ( $\Delta\text{RLU}_{\text{TC}}$ ) was calculated by the following formula:

$$\Delta\text{RLU}_{\text{TC}} = \text{RLU}_{\text{Na}_3\text{VO}_4} - \text{RLU}_{\text{TC}}$$

Where,  $\text{RLU}_{\text{Na}_3\text{VO}_4}$  is the average luminescent light units from  $\text{Na}_3\text{VO}_4$  treated sample and  $\text{RLU}_{\text{TC}}$  is the average luminescent light units from the test compound treated sample. Later, the fold change in ATPase activity was calculated by the following formula:

$$\text{Fold change in P-gp ATPase activity} = \Delta\text{RLU}_{\text{TC}} / \Delta\text{RLU}_{\text{basal}}$$

### 2.3.6. Western blot analysis

Approximately,  $1 \times 10^6$  of KB or KB Ch<sup>R</sup> 8-5 cells were seeded in 100 mm dishes and incubated for 24 hours to retain the morphology. Afterward, the KB Ch<sup>R</sup> 8-5 cells were either treated with

vincristine alone or vincristine in combination with **3** and further incubated at 37 °C under the humidified condition and 5% CO<sub>2</sub>. Cells incubated with just culture media was used as control. After 72 hours of incubation, the cells were lysed and the concentration of protein was estimated by Bradford assay. 30 µg of protein was loaded in each well of a 10% SDS-PAGE and transferred onto the nitrocellulose membrane. The membrane was incubated overnight at 4°C with the corresponding primary antibodies (1:1000 dilution for all). Later, the membrane was washed with TBST (tris buffered saline with 0.1% tween 20) for five times, each wash for five minutes. Consequently, the membrane was incubated either with anti-mouse or anti-rabbit HRP-conjugated secondary antibody (1:5000) for 45 min at room temperature. Later, the membrane was washed with TBST for five times, each wash for five minutes. The bands were visualized by incubating the membrane for two minutes in Clarity Max™ western ECL substrate (Bio-Rad, USA). The membrane was exposed to X-ray films and the relative band intensity was measured using ImagJ software.

### 2.3.7. Statistical analysis

The IC<sub>50</sub> values were determined from the inhibitor concentration vs cytotoxicity response curves in GraphPad Prism 7 (GraphPad Software) using the non-linear regression analysis. For comparison between the groups, one-way analysis of variance (ANOVA) followed by Bonferroni's *post hoc* test was used. Significant changes are indicated as \* p < 0.05, \*\* p < 0.005, \*\*\* p < 0.0005 and \*\*\*\* p < 0.0001.

## 3. Results

### 3.1. *In silico* investigation of piperine analogs

#### 3.1.1. Piperine analogs bind effectively in the drug binding site of P-gp

*In silico* interaction studies of the designed analogs were carried out using human P-gp homology modeled structure. For this, the designed analogs, **3**, **4** and **5**, along with **2** and reference compounds (piperine and verapamil) were docked in the drug binding site of P-gp, to unveil whether they bind in the drug binding site of P-gp with the same affinity as that of **2** and reference compounds. Interestingly, the binding orientation of both **3** and **4** in the drug binding site of P-gp was similar to that of **2**. Moreover, both **3** and **4** showed a lower glide score -9.48 and -9.02 than **2** (glide score -8.42). The glide score of verapamil and piperine was found to be -6.45 and -7.42, respectively (**Fig. 2**).

Whereas, the binding orientation of **5** was found to be different from **2**. The dimethoxy-isoquinoline ring was positioned similar as that in **2**, but the dimethoxybenzene ring was oriented differently, as compared to **2** and the other two analogs **3** and **4**. This could be due to the presence of two bulky methoxy groups in the case of **5**. Moreover, the glide score of **5** was found to be only -7.56. Compounds **3** and **4** showed hydrophobic interactions with the key residues which were found to interact with **2** and the reference compounds (piperine and verapamil). But compound **5** did not show the crucial interactions such as  $\pi$ - $\pi$  interaction with the key residue Phe983 (**Fig. 2** and **Table S1, supporting information**). These results suggest that **3** and **4** have better binding ability in the drug binding site of P-gp and are of more interest for further studies.

### **3.1.2. Piperine analogs show weak interactions in the nucleotide binding domain (NBD) of P-gp**

Compounds that bind in the nucleotide binding domain (NBD) of P-gp would have less specificity and cross-react with other ABC transporters due to the conserved NBD across the ABC transporters. Therefore, to investigate the possibility of piperine analogs (**2**, **3**, **4** and **5**) binding to the NBD of P-gp, the compounds were docked in the NBD1 of modeled human P-gp. All the analogs showed high Glide G-Score compared to ATP, suggesting that they have the least binding ability in the NBD compared to ATP and therefore would preferably bind in the drug binding site of P-gp and exert their action (**Fig. 2**). Thus, these compounds may not cross-react with other ABC transporters as well.

### **3.1.3. Piperine analogs retained interactions with the key residues in the drug binding site of P-gp throughout the molecular dynamics simulation**

To investigate the stability of the P-gp-piperine analogs interaction in the drug binding site, the complex structures were subjected to 100 ns of molecular dynamics (MD) simulation experiments. As P-gp is a membrane bound protein, the P-gp-ligand complexes were embedded in POPC bilayer and simulated as reported by us earlier (Syed et al., 2017). The protein backbone RMSD of P-gp-verapamil, P-gp-piperine, P-gp-**2**, P-gp-**3** and P-gp-**4** varied between 0.5-0.74 nm, 0.4-0.75 nm, 0.5-0.7 nm, 0.5-0.6 nm and 0.6-0.78 nm, respectively (**Fig. 3c**). Further, the RMSD of verapamil alone was found to be 0.2 nm till 10 ns, after that it raised to 0.3 nm and remained in between 0.25 to 0.35 nm during rest of the simulation. Interestingly, the RMSD of piperine and piperine analogs was in the range of 0.1 and 0.25 nm throughout the 100 ns simulation (**Fig. 3c**). The RMSF graph of all the complexes suggests that there was less fluctuation in the drug binding

site residues than that seen in the terminal residues of P-gp (**Fig. S1, supporting information**). Moreover, MM/PBSA based binding free energy calculation showed that both the piperine analogs **3** and **4** have better binding ability to the target than piperine (**Table S1, supporting information**).

Furthermore, to document whether the key hydrophobic interaction between the compounds and drug binding site residues were maintained during the simulations, the initial docked poses, structures extracted from the cluster centre, and the final (at the end of 100 ns MD simulation) protein-ligand complexes were analyzed (**Fig. 3b, Fig. S1, supporting information**). As shown in **Table S1, supporting information**, the majority of the hydrophobic interactions were maintained with all the compounds after the simulation. However, during the simulation process, some of the interactions were lost but some new hydrophobic interactions were formed. This suggests that the protein-ligand complexes were stable and the majority of the interactions were preserved during the simulation. Particularly, compounds **3** and **4** maintained the majority of the hydrophobic interaction with the protein (**Fig. 3b**). Taken together, the results suggest that the ligands were well within the binding pocket throughout the MD simulation.

Overall, *in silico* investigation results suggest that the two newly designed analogs of piperine (**3** and **4**) could interact with the drug binding site of human P-gp protein stably. Therefore, the analogs were synthesized and their biological investigations pursued.

### 3.2. Synthesis of piperine analogs

For the synthesis of **3** and **4**, 4-hydroxy-3-methoxycinnamaldehyde (**6**) was condensed with malonic acid (**7**) under the basic condition to afford the acid intermediate **8** (**Fig. 1**). Treatment of **8** with  $\text{BBr}_3$ , resulted in demethylation product **9**. DIC mediated acid-amine coupling of the acids **8** and **9** with 6,7-dimethoxy-1,2,3,4-tetrahydroisoquinoline (**10**), provided the final products **3** and **4**, respectively. The structure of the products was confirmed by  $^1\text{H}$  NMR and LC-MS spectral data.  $^1\text{H}$  NMR spectra of **3** showed a singlet at  $\delta$  3.94 ppm corresponding to 3 protons, which was not present in the spectra for **4**. This singlet belonged to the methoxy group in the phenyl ring of **3**. Both **3** and **4** were >95% pure as determined by HPLC.

### 3.3. *In vitro* investigation of piperine analogs

#### 3.3.1. Piperine analogs **3** and **4** showed less cross-reactivity with CYP3A4 enzyme

As discussed above, **2** exerted comparatively higher CYP3A4 enzyme inhibition than piperine and verapamil. Therefore, CYP3A4 enzyme inhibitory activity of both **3** and **4** was first investigated to know whether these analogs also cross-reacted with the enzyme. The results showed that both **3** and **4** showed significantly lower CYP3A4 inhibition of 9.6% and 11.1%, respectively at 1  $\mu\text{M}$  and 50% and 54.6% inhibition, respectively at 10  $\mu\text{M}$  concentrations. Moreover, the CYP3A4 inhibitory activity of **3** and **4** was found to be less than that of piperine and verapamil which exerted 21.7% and 24.4% inhibition, respectively at 1  $\mu\text{M}$  and 83.9% and 72.4% enzyme inhibition, respectively at 10  $\mu\text{M}$  concentrations (**Table 1**). Taken together, the results suggest that both **3** and **4** have lower cross-reactivity with CYP3A4, compared to piperine, verapamil and **2** and therefore they have less possibility of interfering with the metabolism of chemotherapeutic drugs. Therefore, the P-gp modulator activity of these two piperine analogs was investigated *in vitro* using P-gp over-expressing cancer cell lines.

### **3.3.2. Dose selection study of 3 and 4 in cancer cell lines**

Compounds which are non-toxic and have no pharmacological activity on their own are considered to be the ideal P-gp inhibitors (Bansal, Akhtar, Jaggi, Khar, & Talegaonkar, 2009). Therefore, in the preliminary study, both KB 3-1 (parental) and KB Ch<sup>R</sup> 8-5 (resistant) cell lines were treated with different concentrations (3.125-100  $\mu\text{M}$ ) of **3** and **4** to determine their non-toxic concentrations. The non-toxic dose could be used for combination studies with a chemotherapeutic drug (vincristine). Based on the results, three non-toxic concentrations (2, 8 and 16  $\mu\text{M}$ ; cell viability > 90%) of **3** and **4** were chosen to study the drug resistance reversal activity in KB cells. Similarly, there was >90% cell viability when the SW480, SW480-VCR, and HCT-15 cells were treated with either **3** or **4**. Therefore, the same non-toxic concentrations (2, 8 and 16  $\mu\text{M}$ ) were fixed to study the drug resistance reversal activity in these cell lines as well.

### **3.3.3. Piperine analogs 3 and 4 exert dose dependent vincristine resistance reversal activity in P-gp over-expressing KB Ch<sup>R</sup> 8-5 cells**

KB 3-1 cells are the parental cells and are sensitive to vincristine. Whereas, the KB Ch<sup>R</sup> 8-5 cells are resistant to vincristine and over-express the P-gp protein (Syed et al., 2017). In order to check the level of vincristine resistance, both KB 3-1 and KB Ch<sup>R</sup> 8-5 cells were treated with different concentrations of vincristine (0.25-8 nM for KB 3-1 and 1.25-160 nM for KB Ch<sup>R</sup> 8-5 cells). The results showed that the IC<sub>50</sub> of vincristine in KB 3-1 (parental) and KB Ch<sup>R</sup> 8-5

(resistant) cells were 1.03 nM and 46.88 nM, suggesting that the KB Ch<sup>R</sup> 8-5 cells were 45.5-fold resistant to vincristine (**Table 2** and **Fig. S2, supporting information**).

Upon co-treatment of KB Ch<sup>R</sup> 8-5 cells with vincristine along with the standard P-gp inhibitor verapamil (2  $\mu$ M), the IC<sub>50</sub> of vincristine was significantly reduced to 4.4 nM, resulting in a 10.5-fold reversal of vincristine resistance. In the previous study, we found that piperine at 2  $\mu$ M concentration could not revert the drug resistance in both KB Ch<sup>R</sup> 8-5 and SW480-VCR cells. Therefore, the concentration of piperine was increased and it was found that at 40  $\mu$ M of piperine co-treatment with vincristine, the IC<sub>50</sub> of vincristine was significantly reduced to 5.43 nM thus caused 8.6-fold reversal of vincristine resistance in KB Ch<sup>R</sup> 8-5 cells and the reversal activity was found to be similar to that of **2** (**Table 2** and **Fig. S2, supporting information**).

Similarly, co-treatment of KB Ch<sup>R</sup> 8-5 cells with vincristine along with **3** (2  $\mu$ M) or **4** (2  $\mu$ M) resulted in a significant increase in the sensitivity of these cells to vincristine and the IC<sub>50</sub> of vincristine was found to be 2.36 nM and 4.68 nM, respectively. Thus, the fold of vincristine drug resistance reversal by **3** and **4** was 11 and 10-fold, respectively. Interestingly, this activity was found to be similar to that of **2** (2  $\mu$ M) which reduced the IC<sub>50</sub> of vincristine to 3.7 nM, thus, caused a 9.7-fold reversal of vincristine resistance in KB Ch<sup>R</sup> 8-5 cells (**Table 2**, and **Fig. S2, supporting information**).

Moreover, increasing the concentration of **3** and **4** caused much more reduction in the IC<sub>50</sub> of vincristine in KB Ch<sup>R</sup> 8-5 cells. In the presence of 8 and 16  $\mu$ M of **3**, the IC<sub>50</sub> of vincristine was significantly reduced to 1.96 and 0.79 nM and thereby reversing the vincristine resistance by 23.9 and 59.3-folds, respectively. Similarly, in the presence of 8 and 16  $\mu$ M of **4** the IC<sub>50</sub> of vincristine was significantly reduced to 2.36 nM and 1.1 nM and caused 19.8 and 42.2-fold reversal of vincristine resistance in KB Ch<sup>R</sup> 8-5 cells, respectively.

To further know whether these analogs also increase the sensitivity of parental cells that were already sensitive to vincristine, KB 3-1 cells were co-treated with vincristine alongside piperine analogs. Interestingly, co-treatment of vincristine along with the highest concentration (16  $\mu$ M) of **3** or **4** showed no significant reduction in the IC<sub>50</sub> of vincristine in KB 3-1 cells. Similar results were obtained when the KB 3-1 cells were co-treated with vincristine alongside verapamil (2  $\mu$ M) or piperine (40  $\mu$ M) (**Table 2** and **Fig. S2, supporting information**). These results suggest that **3** and **4** exert good resistance reversal activity in vincristine resistant KB Ch<sup>R</sup> 8-5 cells; particularly, **3** exerts higher activity than **4**.

### **3.3.4. Piperine analogs 3 and 4 exert dose dependent vincristine resistance reversal activity in P-gp over-expressing colorectal adenocarcinoma cells (SW480-VCR)**

Further, the effect of 3 and 4 was tested in colorectal adenocarcinoma cells SW480 (parental) and in the resistant counterpart SW480-VCR by cell viability assay. The  $IC_{50}$  of vincristine in parental SW480 and resistant SW480-VCR was found to be 2.77 and 48.39 nM, respectively, suggesting that the SW480-VCR cells were 17.5-fold resistant to vincristine (**Table 2 and Fig. S3, supporting information**). Upon co-treatment of resistant cells with vincristine along with verapamil (2  $\mu$ M), the  $IC_{50}$  was significantly reduced to 7.62 nM and caused a 6.35-fold reversal of vincristine resistance in SW480-VCR cells. Co-treatment of resistant cells with vincristine along with 2 (2  $\mu$ M) or 3 (2  $\mu$ M) or 4 (2  $\mu$ M) also caused a significant decrease in the  $IC_{50}$  of vincristine to 21.96 nM or 13.26 nM or 18.32 nM, thus, caused 2.2 or 3.6 or 2.6-fold reversal of vincristine resistance, respectively. However, even the presence of a higher concentration of piperine (40  $\mu$ M) could only reduce the  $IC_{50}$  of vincristine to 23.7 nM, thus caused only a 2-fold vincristine resistance reversal (**Table 2 and Fig. S3, supporting information**).

Interestingly, as observed in KB Ch<sup>R</sup> 8-5 cells, increasing the concentration of 3 or 4 caused much more reduction in the  $IC_{50}$  of vincristine. The observed  $IC_{50}$  of vincristine in the presence of 8  $\mu$ M or 16  $\mu$ M of 3 was 4.68 or 3.52 nM, thereby caused 10.3 or 13.7-fold reversal of vincristine resistance. While in presence of 8  $\mu$ M or 16  $\mu$ M of 4 the  $IC_{50}$  of vincristine was reduced to 7.9 nM or 5.99 nM and caused a 6 or 8-fold reversal of vincristine resistance in SW480-VCR. These results also suggest that both 3 and 4 have better vincristine resistance reversal activity than piperine and 2. Specifically, 3 showed higher resistant reversal activity than all the tested compounds. However, co-treatment of parental SW480 cells with vincristine and piperine analogs showed no significant change in the  $IC_{50}$  of vincristine, similar to that in the case of parental KB 3-1 cells, suggesting that they exert the activity only in the P-gp over-expressing cells (**Table 2 and Fig. S3, supporting information**).

### **3.3.5. Piperine analogs 3 and 4 increase the sensitivity of colon adenocarcinoma cells (HCT-15) to vincristine**

The activity of piperine analogs was further tested in HCT-15 (colon adenocarcinoma) cells which intrinsically express P-glycoprotein (Uchiyama-Kokubu & Watanabe, 2001). The  $IC_{50}$  of vincristine in HCT-15 cells was found to be 294.8 nM (**Fig. S4 and Table S2, supporting information**).

**information**). Upon co-treatment of cells with vincristine and verapamil (2  $\mu$ M), there was an increase in the sensitivity of HCT-15 cells to vincristine and therefore the IC<sub>50</sub> was significantly reduced to 15.8 nM. Similarly, co-treatment of HCT-15 cells with vincristine along with piperine (40  $\mu$ M) significantly reduced the vincristine IC<sub>50</sub> to 51.3 nM. Interestingly, co-treatment of cells with vincristine and **2** (2  $\mu$ M) or **3** (2  $\mu$ M) or **4** (2  $\mu$ M) resulted in a significant change in the IC<sub>50</sub> to 68.7 nM, 42.4 nM, and 46.2 nM, respectively. Moreover, increase in the concentration of **3** or **4** resulted in further reduction of vincristine IC<sub>50</sub> to 14.3 nM and 7.45 nM in the presence of 8  $\mu$ M and 16  $\mu$ M of **3**, 15 nM and 8.5 nM in the presence of 8  $\mu$ M and 16  $\mu$ M of **4**, respectively (**Fig. S4** and **Table S2 supporting information**). The overall results suggest that both **3** and **4** have better drug resistance reversal activity than piperine and **2**, in HCT-15 cells.

### **3.3.6. MRP-1 and BCRP protein inhibitors cause low levels of vincristine resistance reversal in KB Ch<sup>R</sup> 8-5, SW480-VCR and HCT-15 cells**

Apart from P-gp, the other ABC transporters which play an important role in the development of drug resistance in cancer include multidrug resistance associated protein 1 (MRP-1) and breast cancer resistance protein (BCRP) (Stefan, Schmitt, & Wiese, 2017). Therefore, to explore the possible involvement of these transporters in the observed resistance in KB Ch<sup>R</sup> 8-5, SW480-VCR and HCT-15 cells, specific inhibitors probenecid (MRP-1) and novobiocin (BCRP) were used. Upon treatment of KB Ch<sup>R</sup> 8-5 cells with vincristine alone, the IC<sub>50</sub> of vincristine was found to be 46.88 nM. Upon co-treatment of KB Ch<sup>R</sup> 8-5 cells with vincristine along with probenecid (500  $\mu$ M) or novobiocin (50  $\mu$ M), the IC<sub>50</sub> of vincristine was reduced to 25 nM and 31 nM, respectively, compared to the much lower IC<sub>50</sub> of vincristine 4.47 nM when the cells were co-treated with verapamil (2  $\mu$ M) (**Table 3**).

Similarly, the IC<sub>50</sub> of vincristine in SW480-VCR cells was found to be 48.39 nM. Upon co-treatment of vincristine along with probenecid (500  $\mu$ M) or novobiocin (50  $\mu$ M), the IC<sub>50</sub> of vincristine was reduced to only 47.95 nM and 37.66 nM, respectively compared to the much lower IC<sub>50</sub> of vincristine 7.62 nM when the cells were co-treated with verapamil (2  $\mu$ M) (**Table 3**). Likewise, when the HCT-15 cells were treated with vincristine alone the IC<sub>50</sub> of vincristine was found to be 294.8 nM. Upon co-treatment of vincristine along with probenecid (500  $\mu$ M) or novobiocin (50  $\mu$ M) the IC<sub>50</sub> of vincristine was reduced to 137.4 nM and 140.9 nM, respectively, compared to the much lower IC<sub>50</sub> of vincristine 15.82 nM when the cells were co-treated with

verapamil (2  $\mu\text{M}$ ) (**Table 3**). Overall, these results, suggest that the resistance observed in KB Ch<sup>R</sup> 8-5, SW480-VCR and HCT-15 cells is majorly due to the over-expression of P-gp.

### 3.3.7. Piperine analogs 3 and 4 enhanced the ATPase activity of P-gp

In order to explore the possible mechanism of P-gp inhibition by piperine analogs, the effect of these compounds on the ATPase activity of P-gp was assessed. In the absence of any substrate, P-gp has a low ATPase activity which is referred to as the basal ATPase activity. ATPase activity of P-gp increases above the basal activity in the presence of P-gp substrates and decreases below the basal ATPase activity in the presence of P-gp inhibitors that binds to the NBD of P-gp and inhibits its ATPase activity (Lopes et al., 2018).

We observed that when a low concentration (25  $\mu\text{M}$ ) of verapamil (a competitive inhibitor of P-gp) was used, there was only a very little change in the P-gp ATPase activity compared to the basal activity (control). Therefore, the P-gp ATPase activity was monitored at a higher concentration of verapamil (50  $\mu\text{M}$ ) and all other compounds were tested at 25  $\mu\text{M}$  concentration. As shown in **Fig. 4a**, in the presence of verapamil (50  $\mu\text{M}$ ), there was a 1.6-fold increase in the ATPase activity of P-gp compared to the control. Similarly, in the presence of piperine (25  $\mu\text{M}$ ), there was an only 1-fold increase in the P-gp ATPase activity. Whereas, piperine analogs **2**, **3**, and **4** at 25  $\mu\text{M}$  concentration caused a significant increase in the P-gp ATPase activity to 2.5, 2.88 and 2.45-fold, respectively, compared to the control. These results suggest that piperine analogs bind at the drug binding site of P-gp as substrate competitive inhibitors and not at the NBD as ATP competitive inhibitors of P-gp. Specifically, **3** acts as a good substrate competitive inhibitor of P-gp.

### 3.3.8. Piperine analog 3 enhanced vincristine induced NF- $\kappa$ B mediated apoptosis in resistant KB Ch<sup>R</sup> 8-5 cells

NF- $\kappa$ B is a transcription factor that has been reported to alter several cellular functions (Fan, Dutta, Gupta, Fan, & Gélinas, 2008; Park & Hong, 2016). Studies suggest that the activation of NF- $\kappa$ B mediates cell death depending upon the cell type and type of apoptotic stimulus; for instance, treatment with some antineoplastic agents (Barkett & Gilmore, 1999; Buontempo et al., 2016; Das & White, 1997; Farhana, Dawson, & Fontana, 2005; Huang et al., 2004).

Moreover, over-activation of NF- $\kappa$ B has been reported in a large number of drug resistant cancer cell lines and its activation was positively correlated with P-gp expression in these cell

lines (Bentires-Alj et al., 2003; Liu et al., 2014; O'Neill et al., 2011; Xia et al., 2012). Therefore, to document the change in the activation of NF- $\kappa$ B between parental KB 3-1 and resistant KB Ch<sup>R</sup> 8-5 cells, we carried out western blot analysis. Interestingly, the western blot analysis showed that there was a significant increase in the activation of NF- $\kappa$ B p65 (RelA) transcription factor in resistant KB Ch<sup>R</sup> 8-5 cells, compared to the parental cells (**Fig. 4b** and **4c**).

Vincristine produces cytotoxic activity by altering the dynamics of microtubules (Mukhtar, Adhami, & Mukhtar, 2014) and it also induces apoptosis by activating the NF- $\kappa$ B transcription factor (Huang et al., 2004). To better assess if the increase in the sensitivity of KB Ch<sup>R</sup> 8-5 cells to vincristine upon co-treatment with piperine analogs is due to the activation of NF- $\kappa$ B transcription factor, we carried out western blot analysis after co-treating the KB Ch<sup>R</sup> 8-5 cells with vincristine and **3**. As shown in **Fig. 4d** and **4e**, when the KB Ch<sup>R</sup> 8-5 cells were treated with only vincristine (4 nM) there was no alteration in the level of the phosphorylated form of NF- $\kappa$ B. Whereas, co-treatment of cells with vincristine (4 nM) and **3** (2  $\mu$ M) resulted in a significant increase in the phosphorylated form of NF- $\kappa$ B, with a significant decrease in the total NF- $\kappa$ B protein. However, treatment of cells with only **3** resulted in no change in the levels of both total and phosphorylated form of NF- $\kappa$ B. To further document the effect of increased activation of NF- $\kappa$ B on apoptosis, western blot was carried out to detect the levels of both full form and cleaved form of poly-(ADP ribose) polymerase (PARP) protein, a marker for apoptosis induction (Chaitanya, Alexander, & Babu, 2010). As shown in **Fig. 4e**, there was a lower level of cleaved PARP in all the samples including the control, except in the vincristine and **3** co-treated samples, where there was a significant increase in the cleaved PARP.

Taken together, these results suggest that **3** increase the efficacy of vincristine in resistant cells, by increasing the levels of vincristine inside the cells (by inhibiting P-gp efflux), and also induces the NF- $\kappa$ B mediated apoptosis in KB Ch<sup>R</sup> 8-5 cells.

#### 4. Discussion

P-glycoprotein (P-gp/*MDR-1*) plays an important role in the development of multi-drug resistance (MDR) in cancer. Several studies have reported the utility of P-gp inhibitors to overcome MDR when co-administered with various chemotherapeutic drugs (Ghaleb et al., 2018; Waghray & Zhang, 2018). Previously reported P-gp inhibitors were found to have a high molecular weight (>500 Da) and lipophilicity (logP >5). These two physicochemical properties of lead molecules are important, as compounds with high molecular weight and lipophilicity have

higher chances of failure during the drug discovery process (Syed et al., 2017). Therefore, high molecular weight and high lipophilicity of the previous P-gp inhibitors could be one of the possible reasons for their failure in the clinical trials. Another reason for the failure of the previous P-gp inhibitors is their cross-reactivity with cytochrome 450 (CYP) enzymes which metabolize the co-administered chemotherapeutic drugs causing unpredictable toxicities (Wandel et al., 1999). Recently, we identified a low molecular weight and low lipophilicity piperine analog **2** to revert the MDR in P-gp over-expressing cancer cell lines (Syed et al., 2017). However, **2** inhibited CYP3A4 (drug metabolizing) enzyme, suggesting the possibility of interference in the drug metabolism of co-administered chemotherapeutic drugs. Based on our previous results, it is evident that the replacement of piperidine ring of piperine with 6,7-dimethoxytetrahydroisoquinoline ring in **2** enhances the P-gp modulator activity. Therefore, 6,7-dimethoxytetrahydroisoquinoline ring was left unmodified; rather, we attempted to modify the lead **2** at 1,3-benzodioxole (methylenedioxyphenyl) ring to find better P-gp inhibitors with less CYP3A4 inhibitory activity. Further, to support this idea, previous studies have reported that compounds having 1,3-benzodioxole moiety are the most common quasi-irreversible CYP3A4 enzyme inactivators (Orr et al., 2012). Quasi-irreversible inactivation of the CYP enzyme occurs when the reactive species of a compound forms noncovalent interactions with the ferrous form of heme iron atom; this complex is called metabolite intermediate (MI) complex. 1,3-Benzodioxole derivatives form a metabolite intermediate (MI) complex with CYP3A4 through carbene intermediate. The best example reported for Quasi-irreversible inactivator is tadalafil, a phosphodiesterase type 5 inhibitor that is available in the market to treat erectile dysfunction and pulmonary arterial hypertension (Orr et al., 2012). Moreover, some of the phytochemicals (piperine, jatrorrhizine, sanguinarine, etc) having 1,3-benzodioxole ring are also reported to have both P-gp and CYP3A4 inhibitory activity (Bhardwaj et al., 2002; Patil, Gautam, Gairola, Jadhav, & Patwardhan, 2014; Qi et al., 2013).

Therefore, we hypothesized that modifying 1,3-benzodioxole ring may result in relatively less CYP3A4 inhibition. With this aim, three more analogs (**3**, **4**, and **5**) with low molecular weight and lipophilicity were designed based on the lead **2** by opening the 1,3-benzodioxole ring. Replacement of 1,3-benzodioxole ring with 2-methoxyphenol gave **3**, 2-hydroxyphenol gave **4**, and 1,2-dimethoxybenzene gave **5** (**Fig. 1**). Hence, to dial-out the off-target CYP inhibition, 1,3-benzodioxole moiety that is responsible for CYP3A4 enzyme inhibition (Orr et al., 2012) was replaced to design three new low molecular weight and low lipophilic piperine analogs **3**, **4** and **5**.

*In silico* docking studies showed that piperine analog **3** and **4** preferably bind in the drug binding site rather than in the nucleotide binding domain (NBD) of P-gp. It is worth to note that compounds that bind in the NBD of P-gp would also cross-react with other ABC transporters due to the conserved region of NBD across the ABC transporters (Rice, Park, & Pinkett, 2014). It is also suggested that cross-reactivity with other ABC transporters could be one of the reasons for the failure of P-gp inhibitors in the clinical trials (Syed & Coumar, 2016). As piperine analogs preferred to bind to the drug binding site of P-gp, it will have a lower chance of binding to other ABC transporters. Based on the positive findings in the computational study, piperine analogs **3** and **4** were synthesized and tested. Interestingly, the *in vitro* CYP3A4 enzyme activity assay revealed that piperine analogs **3** and **4** exert significantly less inhibitory activity, compared to piperine, verapamil and piperine analog **2**. This could translate to lower interference of piperine analogs **3** and **4** with the drug metabolism of co-administered chemotherapeutic drugs.

In our previous study, we reported the over-expression of P-gp in drug resistant KB Ch<sup>R</sup> 8-5 and SW480-VCR cancer cell lines (Syed et al., 2017). The drug resistance reversal activity of the piperine analogs was tested in these cells. The non-toxic dose of piperine analog **2** was found to be 2  $\mu$ M in KB Ch<sup>R</sup> 8-5 cells, whereas, non-toxic dose of piperine analog **3** and **4** was found to be 25  $\mu$ M. This suggests that the piperine analogs **3** and **4** could be given at higher concentrations as they have less toxicity on their own. It was observed that the P-gp over-expressing KB Ch<sup>R</sup> 8-5 and SW480-VCR cells were 45.52 and 17.46-fold resistant to vincristine, respectively. Interestingly, the presence of piperine analogs **3** and **4** reversed the vincristine resistance in these cell lines and exerted a dose dependent reversal of vincristine resistance. P-gp mediated drug resistance reversal activity of these analogs was seen even at a low concentration (2  $\mu$ M) compared to their CYP3A4 inhibitory concentration (10  $\mu$ M), suggesting that these analogs can be given at lower concentration in combination with chemotherapeutic drugs without affecting their metabolism. At 16  $\mu$ M of piperine analogs **3** and **4** there was a complete reversal of vincristine resistance in KB Ch<sup>R</sup> 8-5 cells and near complete reversal of vincristine resistance in SW480-VCR. On the other hand, these analogs showed no alteration in the sensitivity of parental cells (KB 3-1 and SW480) to vincristine even at higher concentration 16  $\mu$ M, suggesting that these analogs exert their activity only in the drug resistant P-gp overexpressing cancer cell lines. Similarly, **3** and **4** increased the efficacy of vincristine in HCT-15 cells which intrinsically express the P-gp protein, suggesting their role as effective P-gp inhibitors to overcome MDR.

Based on the better drug resistant reversal activity and lower CYP3A4 inhibition, piperine analog **3** was chosen to investigate the molecular mechanism of action in detail. Piperine analog **3** significantly enhanced the P-gp ATPase activity, suggesting it as a competitive inhibitor of P-gp. These results coupled with the *in silico* studies clearly show that **3** binds at the drug binding site and not at the NBD to produce the P-gp inhibition in a competitive manner. Previous studies have reported that over-activation of the transcription factor NF- $\kappa$ B plays an important role in the development of drug resistance in cancer cells, by activating the transcription of P-gp (Bentires-Alj et al., 2003; C. Chen, Shen, Yang, Chen, & Xu, 2011; Q. Chen, Bian, & Zeng, 2014). We found that there was a significant increase in the phosphorylated form of NF- $\kappa$ B p65 in the resistant KB Ch<sup>R</sup> 8-5 cells compared to the parental KB 3-1 cells, suggesting that the activated NF- $\kappa$ B results in overexpression of P-gp. This is in agreement with the previous reports suggesting that the enhanced activation of NF- $\kappa$ B results in overexpression of P-gp (Syed & Coumar, 2016).

Furthermore, western blot analysis revealed that there was no significant change in the phosphorylated form of NF- $\kappa$ B p65 in cells treated with vincristine or piperine analog **3** alone. Whereas, co-treatment of vincristine with piperine analog **3** resulted in a significant increase in the phosphorylated form of NF- $\kappa$ B p65 along with a significant increase in the levels of cleaved PARP, which is a marker of apoptosis induction. This suggests that the co-treatment of piperine analog **3** increased the efficacy of vincristine in KB Ch<sup>R</sup> 8-5 cells, which ultimately induce apoptosis by activating the NF- $\kappa$ B p65 protein.

In conclusion, compared to piperine analog **2**, both piperine analog **3** and **4** have less cross-reactivity with the CYP3A4 enzyme, lower toxicities and exert potent dose dependent drug resistance reversal activity by competitively inhibiting the P-gp function. This would be advantages, as the new piperine analogs (**3** and **4**) would less likely to interfere with the chemotherapeutic drug metabolism during *in vivo* administration. Particularly, **3** ((2*E*,4*E*)-1-(6,7-dimethoxy-3,4-dihydroisoquinolin-2(1*H*)-yl)-5-(4-hydroxy-3-methoxyphenyl)penta-2,4-dien-1-one) can serve as a potential inhibitor of P-gp for *in vivo* investigations in the future, to reverse multi-drug resistance in cancer.

#### Abbreviations

ABC, ATP binding Cassette; CYP3A4, Cytochrome P450 family 3 subfamily A member 4; LCMS, Liquid chromatography mass spectrometry; MDR1, Multidrug resistance protein 1; NF-

$\kappa$ B, Nuclear factor- $\kappa$ B; PARP, Poly adenosine diphosphate ribose polymerase P-gp, P-glycoprotein.

### Data availability

The data that support the findings of this study are openly available in supplementary files (Tables S1, S2; Figures S1, S2, S3, and S4).

### References

- Abdallah, H. M., Al-Abd, A. M., El-Dine, R. S., & El-Halawany, A. M. (2015). P-glycoprotein inhibitors of natural origin as potential tumor chemo-sensitizers: A review. *Journal of Advanced Research*, Vol. 6, pp. 45–62. <https://doi.org/10.1016/j.jare.2014.11.008>
- Bansal, T., Akhtar, N., Jaggi, M., Khar, R. K., & Talegaonkar, S. (2009). Novel formulation approaches for optimising delivery of anticancer drugs based on P-glycoprotein modulation. *Drug Discovery Today*, Vol. 14, pp. 1067–1074. <https://doi.org/10.1016/j.drudis.2009.07.010>
- Barkett, M., & Gilmore, T. D. (1999). Control of apoptosis by Rel/NF- $\kappa$ B transcription factors. *Oncogene*, Vol. 18, pp. 6910–6924. <https://doi.org/10.1038/sj.onc.1203238>
- Becker, J. P., Depret, G., Van Bambeke, F., Tulkens, P. M., & Prévost, M. (2009). Molecular models of human P-glycoprotein in two different catalytic states. *BMC Structural Biology*, 9. <https://doi.org/10.1186/1472-6807-9-3>
- Bentires-Alj, M., Barbu, V., Fillet, M., Chariot, A., Relic, B., Jacobs, N., ... Bours, V. (2003). NF- $\kappa$ B transcription factor induces drug resistance through MDR1 expression in cancer cells. *Oncogene*, 22(1), 90–97. <https://doi.org/10.1038/sj.onc.1206056>
- Bhardwaj, R. K., Glaeser, H., Becquemont, L., Klotz, U., Gupta, S. K., & Fromm, M. F. (2002). Piperine, a major constituent of black pepper, inhibits human P-glycoprotein and CYP3A4. *Journal of Pharmacology and Experimental Therapeutics*, 302(2), 645–650. <https://doi.org/10.1124/jpet.102.034728>
- Buontempo, F., Orsini, E., Lonetti, A., Cappellini, A., Chiarini, F., Evangelisti, C., ... Martelli, A. M. (2016). Synergistic cytotoxic effects of bortezomib and CK2 inhibitor CX-4945 in acute

lymphoblastic leukemia: Turning off the pro-survival ER chaperone BIP/Grp78 and turning on the pro-apoptotic NF- $\kappa$ B. *Oncotarget*, 7(2), 1323–1340. <https://doi.org/10.18632/oncotarget.6361>

Chaitanya, G. V., Alexander, J. S., & Babu, P. P. (2010). PARP-1 cleavage fragments: Signatures of cell-death proteases in neurodegeneration. *Cell Communication and Signaling*, Vol. 8. <https://doi.org/10.1186/1478-811X-8-31>

Chen, C., Shen, H. L., Yang, J., Chen, Q. Y., & Xu, W. L. (2011). Preventing chemoresistance of human breast cancer cell line, MCF-7 with celecoxib. *Journal of Cancer Research and Clinical Oncology*, 137(1), 9–17. <https://doi.org/10.1007/s00432-010-0854-3>

Chen, Q., Bian, Y., & Zeng, S. (2014). Involvement of AP-1 and NF- $\kappa$ B in the up-regulation of P-gp in vinblastine resistant Caco-2 cells. *Drug Metabolism and Pharmacokinetics*, 29(2), 223–226. <https://doi.org/10.2133/dmpk.DMPK-13-SH-068>

Chevillard, S., Pouillart, P., Beldjord, C., Asselain, B., Beuzeboc, P., Magdelénat, H., & Vielh, P. (1996). Sequential assessment of multidrug resistance phenotype and measurement of S-phase fraction as predictive markers of breast cancer response to neoadjuvant chemotherapy. *Cancer*, 77(2), 292–300. [https://doi.org/10.1002/\(SICI\)1097-0142\(19960115\)77:2<292::AID-CNCR11>3.0.CO;2-X](https://doi.org/10.1002/(SICI)1097-0142(19960115)77:2<292::AID-CNCR11>3.0.CO;2-X)

Chung, F. S., Santiago, J. S., De Jesus, M. F. M., Trinidad, C. V., & See, M. F. E. (2016). Disrupting P-glycoprotein function in clinical settings: What can we learn from the fundamental aspects of this transporter? *American Journal of Cancer Research*, Vol. 6, pp. 1583–1598.

Das, K. C., & White, C. W. (1997). Activation of NF- $\kappa$ B by antineoplastic agents. Role of protein kinase C. *Journal of Biological Chemistry*, 272(23), 14914–14920. <https://doi.org/10.1074/jbc.272.23.14914>

Fan, Y., Dutta, J., Gupta, N., Fan, G., & Gélinas, C. (2008). Regulation of programmed cell death by NF- $\kappa$ B and its role in tumorigenesis and therapy. *Advances in Experimental Medicine and Biology*, Vol. 615, pp. 223–250. [https://doi.org/10.1007/978-1-4020-6554-5\\_11](https://doi.org/10.1007/978-1-4020-6554-5_11)

Farhana, L., Dawson, M. I., & Fontana, J. A. (2005). Apoptosis induction by a novel retinoid-related molecule requires nuclear factor- $\kappa$ B activation. *Cancer Research*, 65(11), 4909–4917. <https://doi.org/10.1158/0008-5472.CAN-04-4124>

Ghaleb, H., Li, H., Kairuki, M., Qiu, Q., Bi, X., Liu, C., ... Qian, H. (2018). Design, synthesis and evaluation of a novel series of inhibitors reversing P-glycoprotein-mediated multidrug resistance. *Chemical Biology and Drug Design*. <https://doi.org/10.1111/cbdd.13338>

Huang, Y., Fang, Y., Wu, J., Dziadyk, J., Zhu, X., Sui, M., & Fan, W. (2004). Regulation of Vinca alkaloid-induced apoptosis by NF- $\kappa$ B/I $\kappa$ B pathway in human tumor cells. *Molecular Cancer Therapeutics*, 3(3), 271–277.

Kim, Y., & Chen, J. (2018). Molecular structure of human P-glycoprotein in the ATP-bound, outward-facing conformation. *Science*, 359(6378), 915–919. <https://doi.org/10.1126/science.aar7389>

Kumari, R., Kumar, R., & Lynn, A. (2014). G-mmpbsa -A GROMACS tool for high-throughput MM-PBSA calculations. *Journal of Chemical Information and Modeling*, 54(7), 1951–1962. <https://doi.org/10.1021/ci500020m>

Liu, Z., Duan, Z. J., Chang, J. Y., Zhang, Z. F., Chu, R., Li, Y. N., ... Chang, Q. Y. (2014). Sinomenine sensitizes multidrug-resistant colon cancer cells (Caco-2) to doxorubicin by downregulation of MDR-1 expression. *PLoS ONE*, 9(6). <https://doi.org/10.1371/journal.pone.0098560>

Lopes, A., Martins, E., Silva, R., Pinto, M. M. M., Remião, F., Sousa, E., & Fernandes, C. (2018). Chiral Thioxanthenes as Modulators of P-glycoprotein: Synthesis and Enantioselectivity Studies. *Molecules*, 23(3). <https://doi.org/10.3390/molecules23030626>

Mukhtar, E., Adhami, V. M., & Mukhtar, H. (2014). Targeting microtubules by natural agents for cancer therapy. *Molecular Cancer Therapeutics*, Vol. 13, pp. 275–284. <https://doi.org/10.1158/1535-7163.MCT-13-0791>

O'Neill, A. J., Prencipe, M., Dowling, C., Fan, Y., Mulrane, L., Gallagher, W. M., ... Watson, R. W. G. (2011). Characterisation and manipulation of docetaxel resistant prostate cancer cell

lines. *Molecular Cancer*, 10, 126. <https://doi.org/10.1186/1476-4598-10-126>

Orr, S. T. M., Ripp, S. L., Ballard, T. E., Henderson, J. L., Scott, D. O., Obach, R. S., ... Kalgutkar, A. S. (2012). Mechanism-based inactivation (MBI) of cytochrome P450 enzymes: Structure-activity relationships and discovery strategies to mitigate drug-drug interaction risks. *Journal of Medicinal Chemistry*, Vol. 55, pp. 4896–4933. <https://doi.org/10.1021/jm300065h>

Park, M., & Hong, J. (2016). Roles of NF- $\kappa$ B in Cancer and Inflammatory Diseases and Their Therapeutic Approaches. *Cells*, 5(2), 15. <https://doi.org/10.3390/cells5020015>

Patil, D., Gautam, M., Gairola, S., Jadhav, S., & Patwardhan, B. (2014). Effect of botanical immunomodulators on human CYP3A4 inhibition: Implications for concurrent use as adjuvants in cancer therapy. *Integrative Cancer Therapies*, 13(2), 167–175. <https://doi.org/10.1177/1534735413503551>

Pennock, G. D., Dalton, W. S., Roeske, W. R., Appleton, C. P., Mosley, K., Plezia, P., ... Salmon, S. E. (1991). Systemic toxic effects associated with high-dose verapamil infusion and chemotherapy administration. *Journal of the National Cancer Institute*. <https://doi.org/10.1093/jnci/83.2.105>

Qi, X. Y., Liang, S. C., Ge, G. B., Liu, Y., Dong, P. P., Zhang, J. W., ... Tu, C. X. (2013). Inhibitory effects of sanguinarine on human liver cytochrome P450 enzymes. *Food and Chemical Toxicology*, 56, 392–397. <https://doi.org/10.1016/j.fct.2013.02.054>

Rice, A. J., Park, A., & Pinkett, H. W. (2014). Diversity in ABC transporters: Type I, II and III importers. *Critical Reviews in Biochemistry and Molecular Biology*, Vol. 49, pp. 426–437. <https://doi.org/10.3109/10409238.2014.953626>

Silva, N., Salgueiro, L., Fortuna, A., & Cavaleiro, C. (2016). P-glycoprotein mediated efflux modulators of plant origin: A short review. *Natural Product Communications*, Vol. 11, pp. 699–704.

Stefan, K., Schmitt, S. M., & Wiese, M. (2017). 9-Deazapurines as Broad-Spectrum Inhibitors of the ABC Transport Proteins P-Glycoprotein, Multidrug Resistance-Associated Protein 1, and

Breast Cancer Resistance Protein. *Journal of Medicinal Chemistry*, 60(21), 8758–8780.  
<https://doi.org/10.1021/acs.jmedchem.7b00788>

Syed, S. B., Arya, H., Fu, I. H., Yeh, T. K., Periyasamy, L., Hsieh, H. P., & Coumar, M. S. (2017). Targeting P-glycoprotein: Investigation of piperine analogs for overcoming drug resistance in cancer. *Scientific Reports*, 7(1). <https://doi.org/10.1038/s41598-017-08062-2>

Syed, S. B., & Coumar, M. S. (2016). P-Glycoprotein Mediated Multidrug Resistance Reversal by Phytochemicals: A Review of SAR & Future Perspective for Drug Design. *Current Topics in Medicinal Chemistry*, 16(22), 2484–2508. Retrieved from <http://www.ncbi.nlm.nih.gov/pubmed/26873188>

Tian, P. (2010). Computational protein design, from single domain soluble proteins to membrane proteins. *Chemical Society Reviews*, 39(6), 2071–2082. <https://doi.org/10.1039/b810924a>

Uchiyama-Kokubu, N., & Watanabe, T. (2001). Establishment and characterization of adriamycin-resistant human colorectal adenocarcinoma HCT-15 cell lines with multidrug resistance. *Anti-Cancer Drugs*, 12(9), 769–779. <https://doi.org/10.1097/00001813-200110000-00009>

Waghray, D., & Zhang, Q. (2018). Inhibit or Evade Multidrug Resistance P-Glycoprotein in Cancer Treatment. *Journal of Medicinal Chemistry*, Vol. 61, pp. 5108–5121. <https://doi.org/10.1021/acs.jmedchem.7b01457>

Wandel, C., Richard B, K., Kajiji, S., Guengerich, F. P., Wilkinson, G. R., & Wood, A. J. J. (1999). P-Glycoprotein and cytochrome P-450 3A inhibition: Dissociation of inhibitory potencies. *Cancer Research*, 59(16), 3944–3948.

Xia, Q., Wang, Z. Y., Li, H. Q., Diao, Y. T., Li, X. L., Cui, J., ... Li, H. (2012). Reversion of p-glycoprotein-mediated multidrug resistance in human leukemic cell line by diallyl trisulfide. *Evidence-Based Complementary and Alternative Medicine*, 2012. <https://doi.org/10.1155/2012/719805>

Yao, H. T., Chang, Y. W., Lan, S. J., & Yeh, T. K. (2008). The inhibitory effect of tannic acid on cytochrome P450 enzymes and NADPH-CYP reductase in rat and human liver microsomes. *Food and Chemical Toxicology*, 46(2), 645–653. <https://doi.org/10.1016/j.fct.2007.09.073>

Accepted Article

Yao, H. T., Wu, Y. S., Chang, Y. W., Hsieh, H. P., Chen, W. C., Lan, S. J., ... Yeh, T. K. (2007). Biotransformation of 6-methoxy-3-(3',4',5'-trimethoxy- benzoyl)-1H-indole (BPR0L075), a novel antimicrotubule agent, by mouse, rat, dog, and human liver microsomes. *Drug Metabolism and Disposition*, 35(7), 1042–1049. <https://doi.org/10.1124/dmd.106.014597>

Zhou, D. C., Zittoun, R., & Marie, J. P. (1995). Expression of multidrug resistance-associated protein (MRP) and multidrug resistance (MDR1) genes in acute myeloid leukemia. *Leukemia*, 9(10), 1661–1666.

**Table 1.** Effect of P-gp modulators on CYP3A4 enzyme activity. Azamulin was used as a positive control inhibitor of CYP3A4 enzyme. Data represented as mean  $\pm$  SD of three independent experiments. \*\*  $p < 0.005$ , \*\*\*  $p < 0.0005$  and \*\*\*\*  $p < 0.0001$ , compared to piperine.

Compound	% of CYP3A4 inhibition	
	1 $\mu$ M	10 $\mu$ M
Azamulin	85.5 $\pm$ 0.9****	98.1 $\pm$ 0.1****
Verapamil	24.4 $\pm$ 2.1	72.4 $\pm$ 1.7****
Piperine	21.7 $\pm$ 1.9	83.9 $\pm$ 0.9
2	28.4 $\pm$ 2.4**	92.3 $\pm$ 0.7***
3	9.6 $\pm$ 3.1****	50 $\pm$ 1.6****
4	11.1 $\pm$ 2.5****	54.6 $\pm$ 2.4****

**Table 2.** The effect of piperine analogs on the sensitivity of KB 3-1 (parental), KB Ch<sup>R</sup> 8-5 (resistant), SW480 (parental) and SW480-VCR (resistant) cell lines to vincristine. VCR: Vincristine, Ver: Verapamil, and Pip: Piperine. Data represented as mean ± SD of three independent experiments. \*\*\*\*p< 0.0001 versus vincristine treatment alone.

Treatment	IC <sub>50</sub> (nM) of vincristine					
	KB Cells			SW480 Cells		
	KB 3-1 (Parental)	KB Ch <sup>R</sup> 8-5 (Resistant)	Fold Resistance Reversal (FRR)	SW480 (Parental)	SW480-VCR (Resistant)	Fold resistance reversal (FRR)
<b>Vincristine (VCR)</b>	<b>1.03 ± 0.14</b>	<b>46.88 ± 6.21</b>	<b>0</b>	<b>2.77 ± 0.33</b>	<b>48.39 ± 5.19</b>	<b>0</b>
VCR+ Ver (2 µM)	0.92 ± 0.15	4.47 ± 0.6****	10.48	1.49 ± 0.21	7.62 ± 0.53****	6.35
VCR+ Pip (40 µM)	1.41 ± 0.25	5.43 ± 0.32****	8.63	3.1 ± 1	23.78 ± 3.05****	2.03
VCR+ 2 (2 µM)	0.66 ± 0.16	3.70 ± 0.70****	9.70 (Syed et al., 2017)	2.26 ± 0.61	21.96 ± 1.78****	2.20
VCR+ 3 (2 µM)	-	4.27 ± 0.45****	10.97	-	13.26 ± 1.75****	3.64
VCR+ 3 (8 µM)	-	1.96 ± 0.18****	23.91	-	4.68 ± 0.47****	10.33
VCR+ 3 (16 µM)	0.97 ± 0.27	0.79 ± 0.20****	59.34	1.7 ± 0.4	3.52 ± 0.23****	13.74
VCR+ 4 (2 µM)	-	4.68 ± 0.22****	10.01	-	18.32 ± 1.74****	2.64
VCR+ 4 (8 µM)	-	2.36 ± 0.18****	19.86	-	7.9 ± 0.36****	6.12
VCR+ 4 (16 µM)	1.04 ± 0.19	1.11 ± 0.11****	42.23	1.96 ± 0.25	5.99 ± 0.59****	8.07

**Table 3.** Effect of MRP-1 and BCRP inhibitors on the efficacy of vincristine in resistant cell lines.

\*\*p<0.005 and \*\*\*\* p< 0.0001, versus vincristine treatment alone.

Treatment	Vincristine IC <sub>50</sub> (nM)		
	KB Ch <sup>R</sup> 8-5	SW480-VCR	HCT-15
<b>Vincristine (VCR)</b>	<b>46.88 ± 6.21</b>	<b>48.39 ± 5.19</b>	<b>294.8 ± 108</b>
VCR+ Verapamil (2 μM)	4.47 ± 0.6****	7.62 ± 0.53****	15.82 ± 5.36****
VCR+ Probenecid (500 μM)	25.01 ± 0.89**	47.95 ± 7.49	137.4 ± 30.99
VCR+ Novobiocin (50 μM)	30.99 ± 2.15**	37.66 ± 2.86	140.9 ± 53.73

## Figure Legends

**Fig. 1.** Design of piperine analogs (left panel). Synthesis of piperine analogs **3** and **4** (right panel).

**Fig. 2.** Docking of piperine analogs to drug binding sites and NBD of P-gp. The upper right side panel shows the docking pose of piperine analogs **2** (purple), **3** (green), **4** (magenta) and **5** (yellow) in the drug binding site of P-gp. The binding orientation of both **3** and **4** in the drug binding site is similar to **2**. Whereas, compound **5** orientation is different probably due to the presence of two bulky methoxy groups. Only the key interacting residues are shown for the better visualization of the binding pose. The lower left side panel shows the docking pose of piperine analogs in the NBD and the lower right side panel shows the docking score of these compounds in both the drug binding site and NBD.

**Fig. 3.** Molecular dynamics (MD) simulation (100 ns) of verapamil, piperine, **2**, **3**, and **4** in complex with the human P-gp model. (a) Pictorial representation of the P-gp model embedded in the lipid bilayer used for MD simulation studies. (b) Position of docked compounds (thin grey sticks), and structures at the end of the MD simulation (green). (c) Root mean square deviation (RMSD) graph of the protein backbone and ligands alone.

**Fig. 4.** Effect of verapamil, piperine and piperine analogs on ATPase activity of P-gp (a). The recombinant human P-gp protein in membrane vesicles was either untreated (control) or treated with verapamil (50  $\mu$ M), piperine (25  $\mu$ M), **2** (25  $\mu$ M), **3** (25  $\mu$ M) and **4** (25  $\mu$ M). \* $p < 0.05$  \*\* $p < 0.005$  \*\*\* $p < 0.0001$  versus control (basal ATPase activity). (b and c) representative blot and relative band intensities of NF- $\kappa$ B and p-NF- $\kappa$ B in parental KB 3-1 and resistant KB Ch<sup>R</sup> 8-5 cells, respectively. (d and e) Representative blot and relative band intensities of NF- $\kappa$ B and PARP

Accepted Article

proteins in KB Ch<sup>R</sup> 8-5 cells upon treatment with either vincristine and compound **3** either alone or in combination. The untreated cell lysate served as control. Data represented as mean  $\pm$  SD of three independent experiments. \*\*\*\*p < 0.0001 vs control.

Fig. 1.

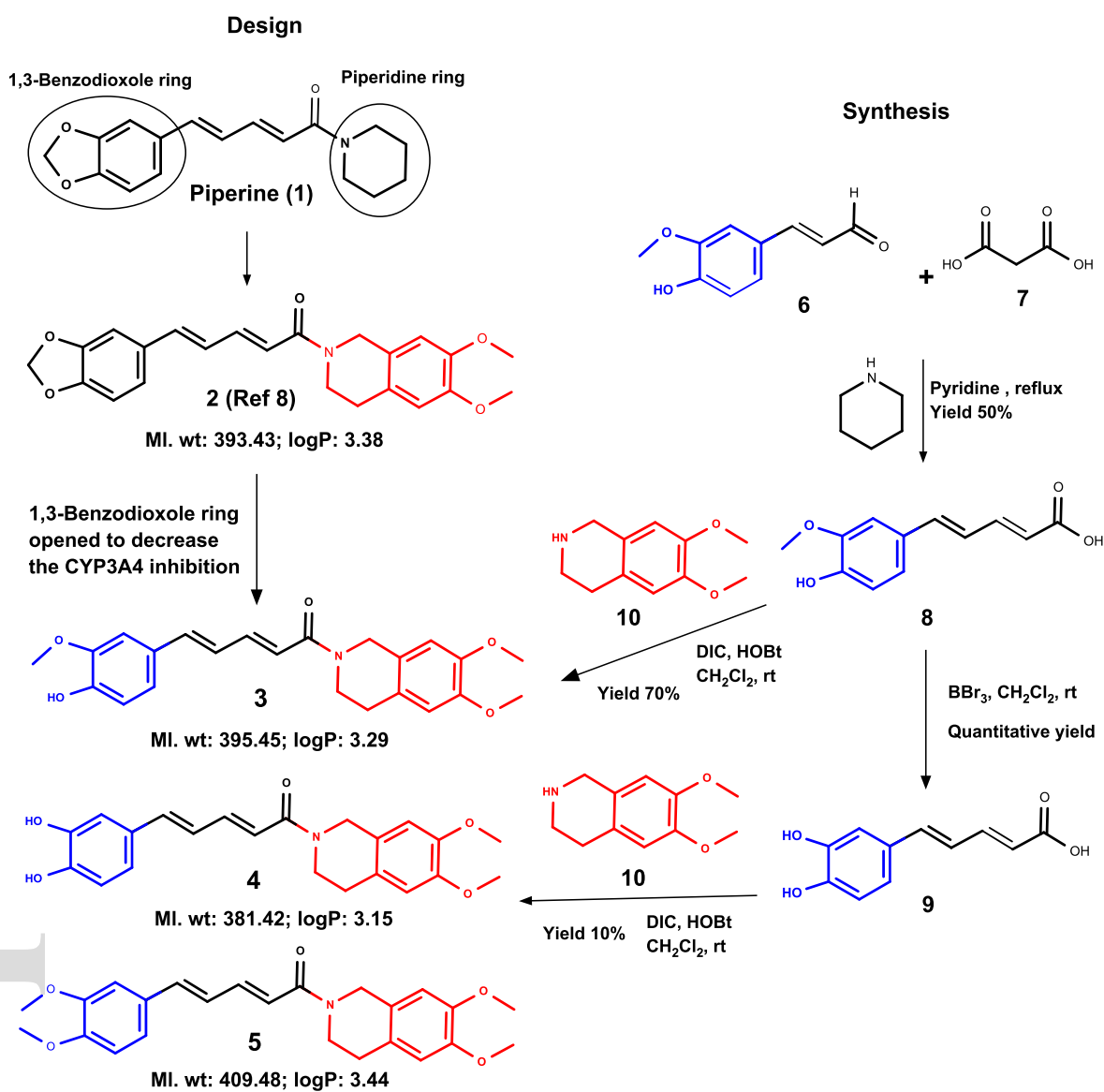


Fig. 2.

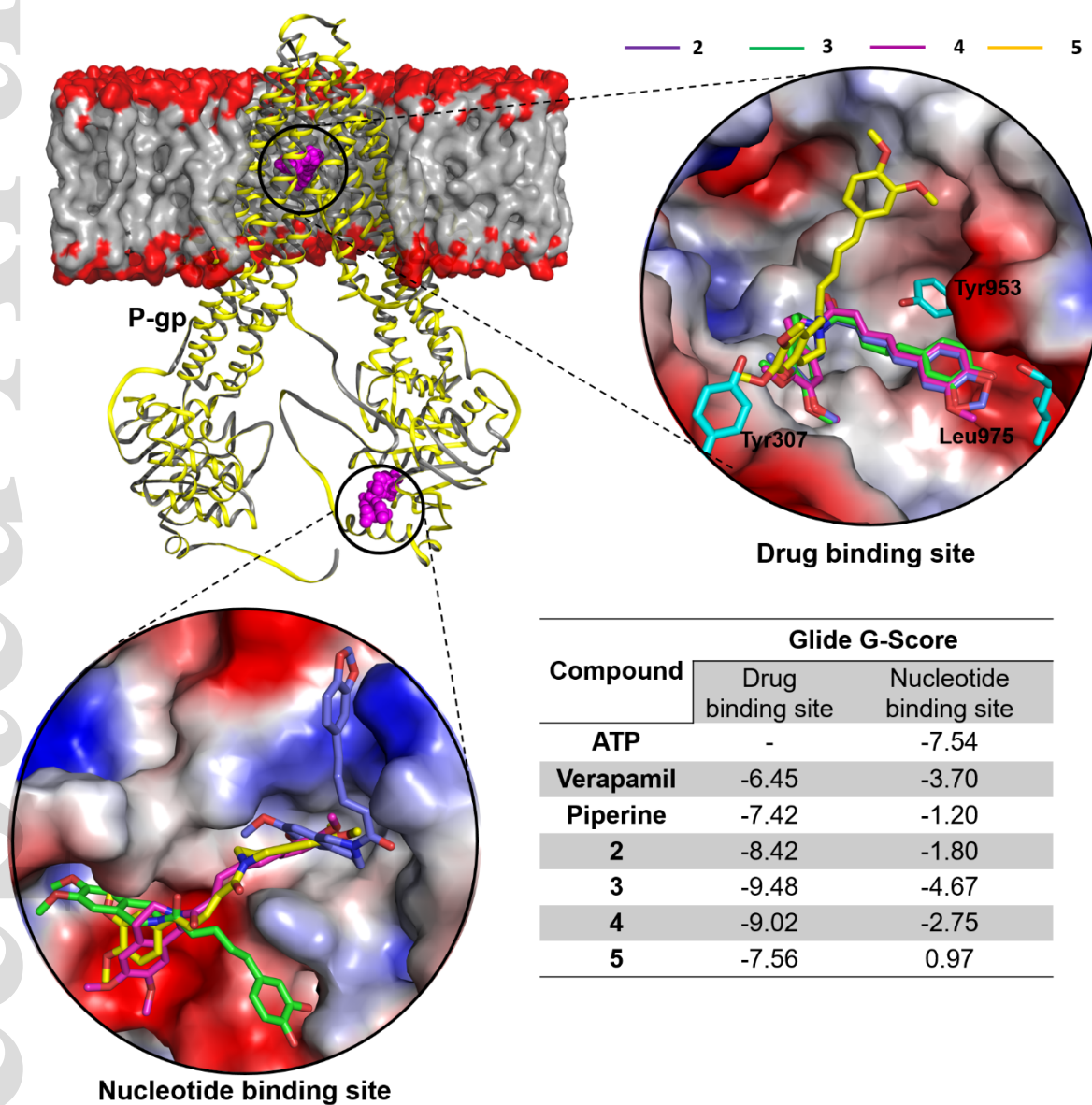


Fig. 3.

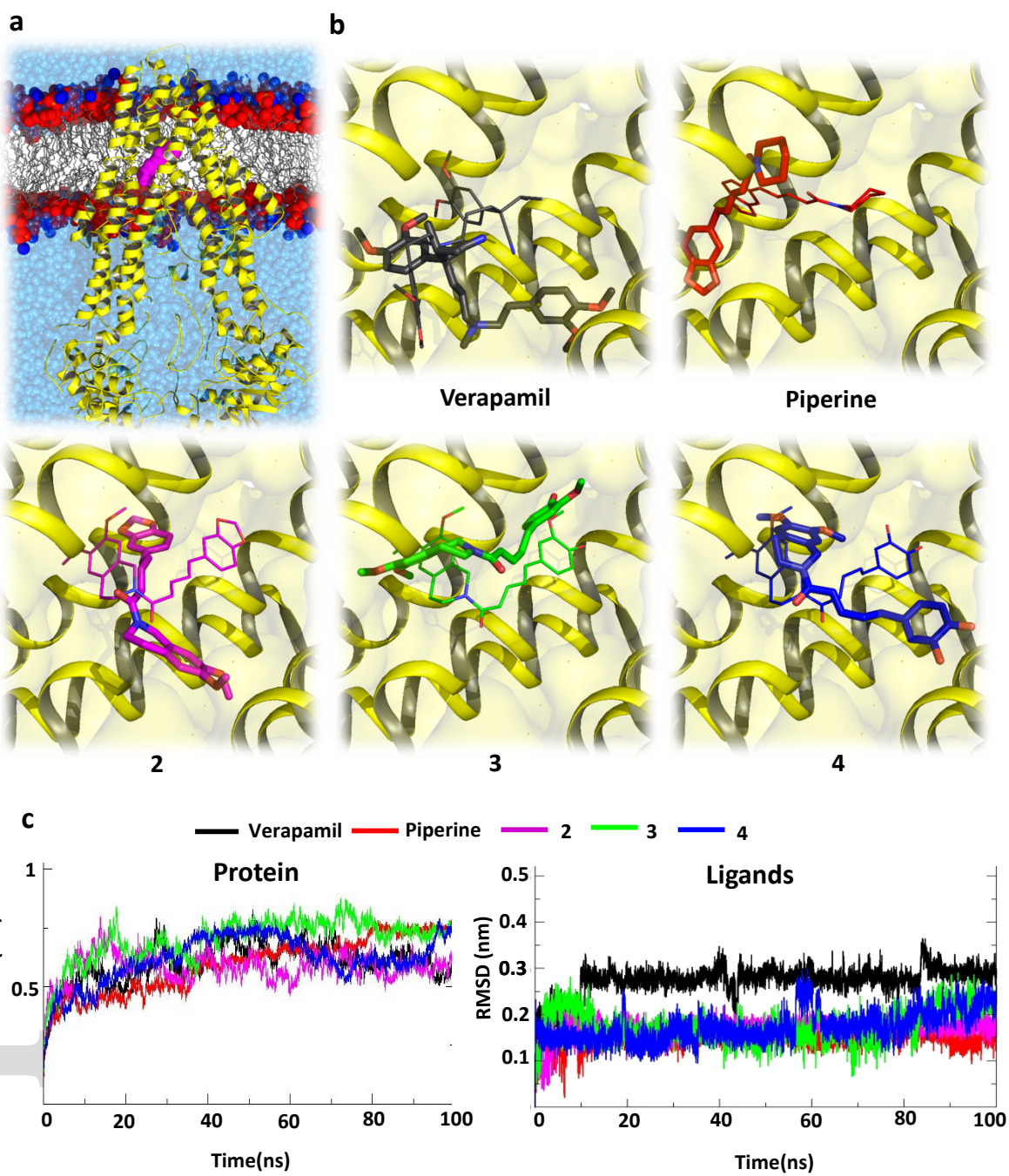


Fig. 4.

